Two-dimensional colloidal aggregation mediated by the range of repulsive interactions

J. C. Fernández-Toledano,[1] A. Moncho-Jordá,[1] F. Martínez-López,[1] A. E. González,[2] and R. Hidalgo-Álvarez[1]
[1]*Grupo de Física de Fluidos y Biocoloides, Departamento de Física Aplicada, Facultad de Ciencias, Campus Fuentenueva S/N, 18071 Granada, Spain*
[2]*Instituto de Ciencias Físicas, Universidad Nacional Autónoma de México, Apartado Postal 48-3, 62251 Cuernavaca, Morelos, México*
(Received 22 December 2006; revised manuscript received 6 February 2007; published 30 April 2007)

We study the effect of the interaction's range on the structural and kinetic properties of a computer-simulated two-dimensional aggregating colloidal system. For this purpose, we considered that the particles of the system interact through a repulsive Yukawa potential which depends on two parameters: the value of the interaction potential between particles in contact V_0 and the range of the interaction κd. We observed that the increase of the interaction range or V_0 provokes the arrangement of the small aggregates in linear structures. The repulsive interactions have also a strong influence on the kinetic behavior of the coagulation process. Indeed, they induce the formation of three different time-separated aggregation regimes. In the first regime (at early states) the aggregation is dominated by the range of the repulsive forces, and the cluster-cluster repulsion increases with the cluster size. The second regime (at intermediate times) is reached when the average cluster size is larger than the interaction range. Here, the cluster-cluster repulsions do not grow anymore with the cluster size, so the probability of overcoming the repulsive barrier is the same for all clusters. This corresponds with the so-called reaction-limited-cluster-aggregation regime, where more than one collision between the clusters is needed to form a bond. The third aggregation regime is found at long aggregation times. In this region the coagulation is mainly determined by the diffusion time and the kinetics becomes diffusion controlled. A physical interpretation for the transition between chain structures and the typical fractals aggregates from the point of view of the range of the interactions is discussed. Moreover, a method has been developed in order to obtain the effect of the interactions with a non-negligible range over the aggregation rates directly from the simulations. The relation between these different regions with the parameters of the interaction potential V_0 and κd is analyzed.

DOI: 10.1103/PhysRevE.75.041408 PACS number(s): 61.43.Hv, 02.70.−c, 82.70.Dd, 05.45.Df

I. INTRODUCTION

Colloidal aggregation is involved in many different applications of the industrial sectors as food technology, biological materials, paintings, polymers, pharmaceutical research, and magnetorheological fluids [1–5]. Moreover, colloidal systems play an important role from the theoretical point of view because they can be used as model systems in order to study complicated physical phenomena such as phase transition [6], multibody interactions [7], and cluster formation of galaxies [8]. Therefore a great effort has been done to understand their main features and to model their aggregation kinetics.

The groundwork for our present understanding of the process of particle aggregation is the result of the work published in 1916 by von Smoluchowski [9]. The Smoluchowski equation describes the kinetic aggregation in terms of the reaction probability (kernel k_{ij}) between clusters of sizes i and j (aggregates composed by i and j monomers, respectively). The physics of the coagulation process is embodied in this reaction probability, which depends on the nature of the relative motion between the aggregates as well as the details of the pairwise interaction potential among the clusters.

In the last decade, both theories and experiments have shown the existence of two universal behaviors, independent of the particle nature, called diffusion-limited cluster aggregation (DLCA) or reaction-limited cluster aggregation (RLCA). The better known aggregation kinetics corresponds to the DLCA regime [10]. In this case, colloidal particles freely move by Brownian diffusion (without interparticle interactions) and they become irreversibly stuck after a collision. The kinetic properties of this aggregation process have been described using the Brownian kernel [11].

Another studied aggregation regime corresponds to colloidal particles that experience short-range interparticle repulsions. These repulsions provoke a decrease of the aggregation rate. When the potential barrier is short-ranged (compared to the particle radius), the interaction between the particles is approximated by a sticking probability defined as the fraction of effective collisions leading to the formation of new bonds. This is usually called the reaction-limited cluster aggregation (RLCA) regime [12,13].

However, when the range of the repulsive interactions is not negligible, the aggregation process cannot be modeled in terms of the sticking probability. It is necessary to include the effect of the interaction range in the aggregation kernels in order to describe properly the kinetics of the aggregation process.

A previous simulation work (Ref. [14]), using a Metropolis Monte Carlo procedure, was able to successfully obtain the low cluster fractal dimensions obtained experimentally on a two-dimensional colloidal aggregating system [15], whose particles were supposed to interact via a repulsive medium-range potential. However, that work was restricted to the structural behavior, while the dynamics was set aside. Furthermore, due to computational limitations, the simulations were stopped at a short time, preventing us from seeing the crossover that is generally known to occur from RLCA to DLCA, due to the multiple contacts that two large colliding clusters can have.

In this paper we report the effect of the medium-range repulsive interactions on the kinetic and structural properties of the aggregating clusters in simulations of colloidal particles whose movement is confined into a plane. This work gives the answer to an important question: how the aggregation rate and the cluster structure of two-dimensional coagulation are affected by the presence of a repulsive component with a non-negligible range in the total interaction potential? The repulsive interaction considered is the Yukawa potential, which has been used in many fields to model screened interactions.

The paper is organized as follows. Section I is the introduction. Section II reviews the theoretical background needed for describing the aggregation kinetics when the particles interact through a pairwise interaction potential with a non-negligible range. Section III describes the simulations. Section IV summarizes the results of the simulations and the discussion. Finally, the main conclusions are extracted in Sec. V.

II. THEORETICAL BACKGROUND

A. Cluster structure

The observations that the structure of clusters formed during an aggregation process exhibit fractal behavior, at least within certain length scales, have substantially simplified the description of the cluster geometry. The fundamental relation is the scaling of the cluster size i with its cluster radius of gyration (R_g):

$$R_g \sim i^{1/d_f}, \quad i \gg 1, \tag{1}$$

where d_f is the fractal dimension and $iR_g^2(i)=\langle\Sigma_{k=1}^{i}[(x_k-x_{\text{c.m.}})^2+(y_k-y_{\text{c.m.}})^2]\rangle$ (c.m. indicates the position of the center of mass of the cluster and k denotes the position of the particles in a cluster of size i).

The fractal dimension characterizes the inner structure of the cluster and it depends on both the clusters-diffusion and the cluster-cluster interaction. As it is well-known, DLCA aggregation leads to more open structures ($d_f \approx 1.44$ for 2D-DLCA) than in the case of short-range likely repulsion, e.g., RLCA regime ($d_f \approx 1.55$) [16]. For RLCA aggregation regime multiple collisions between two clusters are required to coagulate them. The probability of coagulation in this regime is proportional to the number of collisions. Therefore a higher interpenetration between clusters is necessary, which provides a greater number of potential monomer-monomer combinations. This fact explains the formation of more compact aggregates under the RLCA regime in comparison with those formed under the DLCA regime.

B. Kinetics

The most important quantities that characterizes the kinetic properties of a coagulating system is the cluster size distribution $n_i(t)$ defined as the number of clusters containing i monomers at time t. The time evolution of the aggregation process is featured in global terms using the weight-average cluster size $S_w(t)$ given by [17]

$$S_w(t) = \frac{\sum_{i=1}^{\infty} i^2 n_i(t)}{\sum_{i=1}^{\infty} i n_i(t)}. \tag{2}$$

For long aggregation times, it has been observed experimentally and by simulations that the weight-average cluster size develops a power-law behavior for long times, $S_w(t) \sim t^z$, where z is the so-called kinetic exponent. Then, if one represents the function $S_w(t)^2 n_i(t)$ versus a normalized cluster size, $i/S_w(t)$, we see that all the curves can be scaled into a single time-independent scaling function $\Psi[i/S_w(t)] = S_w(t)^2 n_i(t)$. The shape of this master curve depends on the aggregation regime [18,19].

For dilute systems, the time evolution of the cluster populations is given by the Smoluchowski equation [9]:

$$\frac{dc_k(t)}{dt} = \frac{1}{2}\sum_{i+j=k} k_{ij} c_i(t) c_j(t) - \sum_{j=1}^{\infty} k_{kj} c_k(t) c_j(t). \tag{3}$$

Here, $c_i(t)$ are the cluster concentrations defined as $c_i(t) = n_i(t)/S$, where S is the total area of the system. This is a mean-rate equation that predicts the evolution of the mass spectrum of a collection of particles due to successive mergers. It is widely used for modeling growth in many fields of science. Examples include planetesimal accumulation, mergers in dense clusters of stars, coalescence of interstellar dust grains, galaxy mergers in astrophysics, aerosol coalescence in atmospheric physics, colloids, and polymerization and gelation [20–23]. The first term of Eq. (3) accounts for the creations of k-mers through collision of j-mers and $(k\text{-}j)$-mers and the second term represents the annihilation of k-mers due to a coagulation with other clusters.

Equation (3) gives the kinetic aggregation in terms of the reaction kernel k_{ij}, which is related to the aggregation rate between an i-mer and a j-mer. The reaction kernel accounts for two physical factors: the collision frequency between two clusters and the corresponding sticking efficiency.

Some approximations are involved in this equation: first, it considers only binary collisions. Second, the aggregation is irreversible, i.e., the possibility of fragmentation or rearrangement of the particles in the aggregate is not taken into account. Third, the effect of cluster morphology on the rates of aggregation is averaged over all particular cluster formation possibilities. Finally, we assume that there are no spatial correlations between the clusters. So, this equation is a mean field approach to the aggregation dynamics.

A more general and realistic description of the aggregation process should include the possibility that the aggregates could break into smaller pieces or rearrangement. This is the well-known reversible aggregation process, which has been the subject of extensive theoretical and computational work [24,25]. However, the experimental results for two-dimensional coagulation processes showed than the bonds formed by aggregation are very rigid and this reversible aggregation has not been observed yet. Therefore we only considered irreversible aggregation in this work.

The Smoluchowski equation gives the time evolution of the cluster concentration in terms of the reacting kernels, k_{ij}, which is related to the aggregation rate between i-mers and j-mers. Most kernels used in the literature are homogeneous functions of i and j. According to van Dongen and Ernst [26], this kind of kernel may be characterized by two exponents, λ and μ, which are defined as

$$k_{ai,aj} = a^{\lambda} k_{ij}, \quad i,j \gg 1,$$

$$k_{ij} \sim i^{\mu} j^{\lambda-\mu}, \quad j \gg i, \tag{4}$$

where a is a large positive constant. For $\lambda < 1$, the exponents z and λ are related by $z = 1/(1-\lambda)$.

The aggregation kernel is directly related to the "average lifetime" $\langle t_{ij} \rangle$, which represents the mean time used by aggregates of sizes i and j to diffuse and coagulate:

$$k_{ij} \sim \frac{1}{\langle t_{ij} \rangle}. \tag{5}$$

For certain aggregation kernels an analytical solution as well as scaling solutions of Eq. (3) are available [11,27]. However, in the general case only numerical solutions can be obtained.

When clusters stick at the first collision, the aggregation rate is completely determined by the Brownian diffusion of the aggregates (DLCA). For this regime, an explicit expression for the kernel may be obtained by estimating the rate of collisions for sufficiently long times. In a d-dimensional space, this reasoning yields [28]

$$k_{ij}^{Br} \sim (D_i + D_j)(R_i + R_j)^{d-2}, \tag{6}$$

where D_i and R_i are the diffusion coefficient and the radius of gyration of an i-size aggregate, respectively.

We assume that the average diffusion coefficient for a cluster with a characteristic radius of gyration R_g is given by $D \sim 1/R_g$ [29]. Inserting here Eq. (1), one finally obtains for $d=2$:

$$k_{ij}^{Br} = \frac{k_{11}^{Br}}{2}(i^{-1/d_f} + j^{-1/d_f}). \tag{7}$$

This kernel is homogeneous, having $\lambda = \mu = -1/d_f = -1/1.45 \approx -0.69$.

When repulsive interparticle forces are present, the aggregation rate decreases since only a fraction of the cluster-cluster collisions leads to coagulation. In this case, the interaction kernel, k_{ij}, can be written as

$$k_{ij} = \frac{k_{ij}^{Br}}{W_{ij}} = k_{ij}^{Br} P_{ij}, \tag{8}$$

where the stability factor W_{ij} is the stability factor defined as the ratio of the aggregation rate constants for noninteracting particles and for those with a finite interaction. W_{ij} is a measure of the stability of the colloidal dispersions. Analogously, P_{ij} represents an effective sticking probability. Fuchs [30] derived the following relationship between the total interaction potential $V_{ij}(r)$ and the stability factor in a three-dimensional coagulation process:

$$W_{ij} = [R_g(i) + R_g(j)] \int_{R_g(i)+R_g(j)}^{\infty} \frac{\exp[V_{ij}(r)/k_B T]}{r^2} dr. \tag{9}$$

If $V_{ij}(r)$ is a short-range repulsive interaction, the kinetic coagulation regime corresponds to RLCA. In this case, the P_{ij} functions increase with the cluster size because the probability of collision of two aggregates grows with the number of particles that can collide. The characteristic kernel used in this regime is [12]

$$k_{ij} = k_{ij}^{Br} P_0 (ij)^{\lambda}. \tag{10}$$

The λ parameter accounts for the increased aggregation efficiency of larger clusters due to a larger number of contact possibilities on their surface and P_0 is the monomer-monomer sticking probability.

It is worth noting that, in the absence of attractive interaction between the particles, the DLCA regime represents the upper limit of the cluster aggregation rate constant. The number of consecutive collisions between two aggregates increases for larger cluster sizes. This implies that two huge approaching clusters are involved in so many consecutive collisions that, even for very low sticking probabilities, they are not able to diffuse away and finally end up forming a stable bond. This corresponds to the transition from RLCA to DLCA, which occurs as the aggregate size increases in time and it has been experimentally observed [31–33] and theoretically modeled [16,33].

C. Effect of the interaction range

The effect of the interaction range over the coagulation process could be explained on the basis of the "superposition principle" applied to find the cluster-cluster interaction potential. This potential can be obtained as the sum of all the interactions between the monomers that compose the interacting aggregates. Therefore the total interaction between an i-mer and a j-mer can be estimated with the following formula:

$$V_{ij} = \sum_{k=1}^{i} \sum_{m=1}^{j} V_{11}(r_{km}), \tag{11}$$

where $V_{11}(r)$ is the monomer-monomer interaction potential and r_{km} is the center-to-center distance between the k-monomer of the i-cluster and the m-monomer of the j-cluster.

It is not possible to define a collision between two clusters as usual, when we have colloidal particles that interact among them through a potential with a non-negligible interaction range. In this case, two approximating clusters feel each other before and after they collide. For this reason, it is necessary to define an interaction region between two monomers as a circle of radii r_{cut} centered in one of the monomers where $V_{11}(r > r_{cut}) < 0.1 k_B T$. Hence the monomer-monomer interaction outside of this region, i.e., when the distance between the centers of the monomers is larger than r_{cut}, can be considered negligible. The monomers are depicted as gray disks in Fig. 1. Around one of theses monomers the "interaction region" is sketched as a dashed circle of radii r_{cut}.

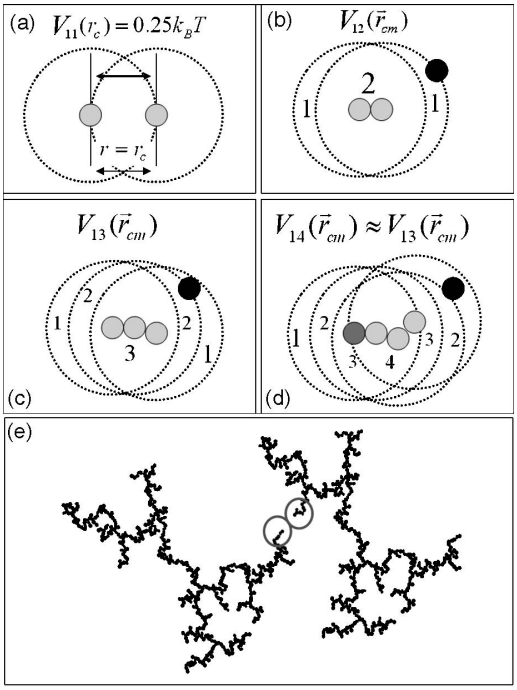

FIG. 1. Scheme of cluster-cluster interactions. The monomers are represented as gray disks and the interaction region around a monomer is sketched as a dashed circle. (a) The monomer-monomer interaction is isotropic. When one of the monomers is outside the interaction region of the other monomer, the interaction potential is neglected. (b) The dimer-monomer interaction is anisotropic. Around the dimer there is a more repulsive region due to the superposition of two monomer-monomer interactions (denoted as $I=2$ in this scheme) and a less repulsive region ($I=1$). (c) Trimer-monomer interaction. The interaction is again anisotropic and it is easier to induce coagulation at the extremes of the trimer. (d) Tetramer-monomer interaction. In this scheme, not all the monomers being part of the same tetramer participate in the interaction as the monomer cannot "feel" the gray particle of the tetramer. (e) Cluster-cluster interaction. Only the monomers that are inside the circles participate in the interaction.

Now, we define an "encounter" between two clusters which begins when any monomer of one aggregate crosses the interaction region of some monomer of the other aggregate. The encounter finishes when these clusters coagulate or when one of the aggregates diffuses away from the interaction region of the other. It may now have a new encounter with another cluster.

A dimer is formed when the monomers overcome the repulsive barrier and they collide, forming a strong bond arising, in the true experimental colloidal system, from the van der Waals interactions. This strong bond would not allow each of the particles to roll over around the other, due to the roughness of their surfaces. In Fig. 1(b) we represent the interaction between a dimer and a monomer. As the interaction range is larger than the particle diameter, there is some region around the dimer where the interaction is summed due to the superposition principle. Therefore we can distinguish two different regions in a dimer: a more repulsive region [depicted as $I=2$ in Fig. 1(b)] due to the overlapping of the repulsive interactions of the two monomers that compose the dimer, and a less repulsive region [depicted as $I=1$ in Fig. 1(b)] where there is no overlapping of the interaction regions. Hence the resulting interaction potential V_{12} is anisotropic, which means that when a monomer interacts with a dimer, there is a convenient orientation between the aggregates which minimizes the repulsive interaction. So, the coagulation is easier when they approach through the less repulsive region $I=1$.

With the same idea, three different spatial regions appear when a trimer interacts with a monomer, depending on the number of superposed monomer-monomer interactions. In Fig. 1(c) they are represented as $I=1$, 2, and 3. Again, the aggregation will occur preferentially through a low-number region (less repulsive region). The $I=1$ regions are usually at the extremes of the aggregates, so it is easier for a monomer to coagulate in such extremes, and therefore the small aggregates tend to develop a linear structure (chains).

In the case of the tetramer-monomer interaction [Fig. 1(d)], it is possible for the monomer to coagulate through an interaction region $I<4$. This means that not all the monomers forming part of the tetramer participate in the interaction (the monomer can aggregate with the tetramer without feeling the interaction of the whole cluster). Therefore we can define the critical cluster size, i_0, as the maximum size in which all the monomers forming the cluster participate in the interaction with the approaching monomer.

Hence the interaction between a monomer and a cluster of size i becomes more repulsive with the increasing of i until it reaches the critical size i_0. After that, the monomer-cluster interaction becomes independent on the cluster size.

When two clusters larger than the critical size approach each other, not all the monomers participate in the interaction. From this moment, there is not any "privileged" direction and the aggregates with a size $i>i_0$ begin to lose their linearity. In Fig. 1(e) two interacting big aggregates are shown. In this case, the monomers that participate in the interactions are the monomers inside the circles. Therefore when the colloidal particles interact between them through a potential with a non-negligible range (in comparison with the particle diameter), we will have the following kinetic regions.

First region. For small aggregates, the cluster-cluster repulsions increase with the cluster size due to the superposition of the interactions. Therefore the function P_{ij} of Eq. (8) decreases with the clusters size. In this region, the cluster-cluster interaction is anisotropic and this causes the formation of chains, which is the preferred configuration to minimize the repulsive interaction between two approaching clusters.

Second region. When the size of the interacting clusters is bigger than the critical size, i_0, the cluster-cluster interaction potential becomes size independent since not all the monomers that form the aggregates participate in the interaction. Since the range of the cluster-cluster interactions do not grow anymore with the cluster size, the probability of overlapping the repulsive barrier tends to be also size-independent. Under this situation we can use again the term "collision" between clusters. Moreover, the interaction is more isotropic than in the previous region and the chains coagulate to form clusters with higher fractal dimension. Al-

though the collision efficiencies are constant, the probability P_{ij} of coagulation of two clusters with sizes larger than i_0 still grows with the size, due to the increase of the cluster cross section. Hence the typical coagulation kinetics for the RLCA regime [kernel of Eq. (10)] is recovered.

Third region. For long enough aggregation times, the cross section of the clusters is so large that the number of consecutive collisions per encounter between a pair of neighboring clusters is usually very high. This implies that two colliding big clusters are not able to diffuse away and finally end up forming a bond. Hence in this region a cluster coagulates almost certainly during its first encounter with another cluster and the aggregation rate becomes diffusion controlled (DLCA). However, there is a finite time between the encounter and the coagulation that prevents reaching completely the DLCA regime. Therefore the kernel for this third region will be

$$k_{ij} = A k_{ij}^{Br}, \tag{12}$$

where A is a constant with values $0 \leqslant A \leqslant 1$.

Hence the coagulation of the large clusters is controlled by the Brownian diffusion of the aggregates, and then the kinetic exponent z of Eq. (2) and the fractal structure of the final clusters will be the same as in a typical DLCA coagulation regime.

III. SIMULATIONS DESCRIPTION

A. Simulation sketch

Brownian dynamics off-lattice simulations were performed in a square box of side L, by considering a total number of monomers of $N_0=20\,000$ with a particle radius $a=300$ nm and a packing fraction of $\phi_s=N_0\pi a^2/L^2=0.001$. In the initial state, monomers were placed at random avoiding particle-particle overlapping. Periodic boundary conditions were imposed at the boundaries of the simulation surface. The time step of the simulation Δt was constant and the mean square displacement of a particle is $2\sqrt{k_B T \Delta t/(3\pi\eta a)}$. This simulation was designed to model a two-dimensional system of bare colloidal particles, capable of truly irreversible aggregating in a very deep and very short-ranged primary minimum coming from the van der Waals interactions between the colloidal particles, as described in the DLVO theory. This aggregation would take place as long as the particles are capable of surmounting (by thermal fluctuations) the repulsive potential barrier, whose height and range are explicitly varied in our simulations.

The interaction potential between the particles considered in the simulations was the Yukawa potential:

$$V_{11} = \frac{V_0}{r} e^{-\kappa d(r-1)}, \tag{13}$$

where r is the distance between the centers of the particles expressed in units of the particle diameter $d=2a$, V_0 is the potential between particles in contact ($r=1$), and $1/(\kappa d)$ is related to the range of the potential (see Fig. 2). As the purpose of this work is to study the effect of the repulsive part of the potential when this is long-or medium-ranged, of more than a particle radius, we did not consider the possibility of having a secondary minimum after the potential barrier, coming from the van der Waals attraction.

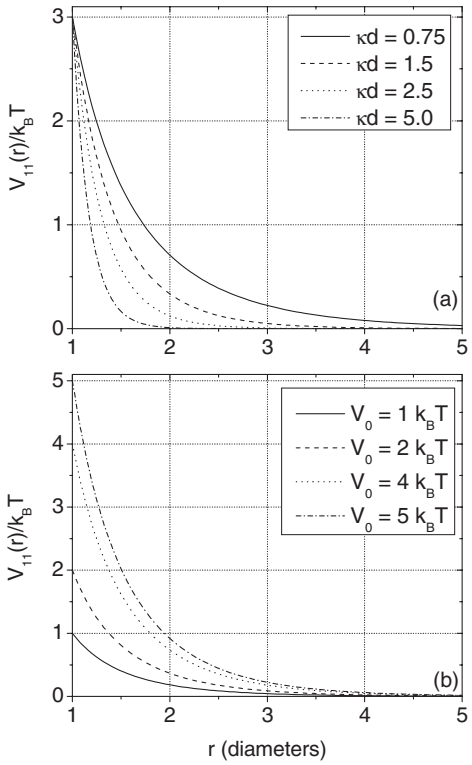

FIG. 2. Interaction potentials used in the simulations. (a) Different interaction ranges (κd) used ($V_0=3k_BT$). (b) Different V_0 values used ($\kappa d=1$).

The movement of the aggregates in the simulation is performed as follows: one of the clusters is picked cyclically and the deterministic total force $\vec{F}_{ext}$ acting over it is calculated. This total force is the result of the pairwise Yukawa interaction [Eq. (13)] with the particles of other clusters that are closer than the cutoff length r_{cut}. This cuttoff length was taken in order to have $V_{11}(r_{cut})=0.1k_BT$,

$$\vec{F}_{ext} = -\sum_{particles} \vec{\nabla} V_{11}. \tag{14}$$

The particle motion is governed by the Langevin equation [34]:

$$\frac{d\vec{p}}{dt} = -\vec{F}_f + \vec{f} + \vec{F}_{ext}, \tag{15}$$

where $\vec{f}(t)$ is a rapidly varying force resulting from the random collisions of the solvent molecules with the cluster, and $\vec{F}_f$ is the frictional force due to the systematic collisions with the solvent molecules as the cluster moves, which depends on the cluster velocity.

Equation (15) is solvable and the probability density function in the diffusive time scale, defined as the probability to find a cluster at the position $\vec{r}$ at time t, given that it was in $\vec{r}_0$ at time t_0, is given by

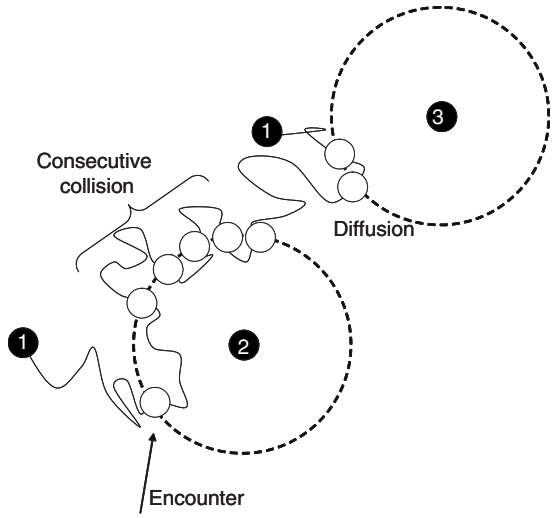

FIG. 3. In this scheme we depicted three monomers labeled as 1, 2, and 3. The dashed circles around the monomers 2 and 3 of radii r_{cut} represent the interaction regions around them. Outside this region, the monomer-monomer interaction is negligible $[V_{11}(r > r_{cut}) < 0.1k_BT]$. First, the particle 1 crosses the interaction region of particle 2 several times (first encounter). This encounter finishes when particle 1 diffuses away from particle 2 to interact with particle 3.

$$P(\vec{r},t) = \frac{1}{4\pi D\Delta t} e^{-|\vec{r} - \vec{r}_0 - \vec{F_{ext}} t/\gamma|^2/(4D\Delta t)}, \tag{16}$$

where D is the cluster's diffusion coefficient, $1/\gamma = D/(k_BT)$, k_B is the Boltzmann constant, and T is the temperature. The center of mass of the cluster is moved by a vector $\vec{d} = (d_x, d_y)$ where d_x and d_y are numbers distributed according to this Gaussian probability distribution.

A coagulation is considered to occur when a moved aggregate overlaps another one. Then, the position of the moved cluster is corrected in the opposite direction of movement, putting them in contact. Afterwards, these clusters are joined to form a larger cluster that will continue the movement in the following time step.

The simulations were stopped when the number of clusters was smaller than 200 aggregates. For the entire simulations performed, this condition is enough to reach the scaling time and it is a warranty to have good statistics for all aggregation times. The algorithms used in this work have been already applied with success to prove the existence of dynamic scaling in both DLCA and RLCA regimes [16,35,36].

B. Method to obtain the aggregation kernel

In order to describe the kinetics of a coagulation process we have developed a method to obtain the ratios k_{ij}/k_{ij}^{Br} directly from the simulations performed. In all simulations we associated to each monomer an interaction region as a circle centered on it of radius r_{cut} (Fig. 3). The interaction potential with another monomer outside this region is neglected $[V_{11}(r > r_{cut}) < 0.1k_BT]$. We define N_{ij} as the average number of encounters between clusters of size i with clusters of size j, and C_{ij} as the number of coagulations between i-clusters with j-clusters. Therefore we can calculate the "probability of coagulation per encounter" $(\mathcal{E}_{ij})$ as

$$\mathcal{E}_{ij} = \frac{C_{ij}}{N_{ij}}. \tag{17}$$

If we keep the same cutoff radius, r_{cut}, for the DLCA coagulation process we have that $\mathcal{E}_{ij}^{DLCA} < 1$ because not all encounters lead to coagulation. In order to consider only the effect of the interaction potential (not the diffusion effect), we need to discount the probability of coagulation by encounter due to pure diffusion $\mathcal{E}_{ij}^{DLCA}$ (without interactions). Therefore the probabilities P_{ij} may be obtained as the ratio

$$P_{ij} = \frac{\mathcal{E}_{ij}}{\mathcal{E}_{ij}^{DLCA}} = \frac{k_{ij}}{k_{ij}^{Br}}. \tag{18}$$

Hence with the Brownian kernel of Eq. (7) and the values of P_{ij} calculated from the simulations, we obtain the coagulation kernel. Therefore we are able to study directly the effect of the variation of the different parameters of the interaction potential over the coagulation rates.

C. Method to solve the Smoluchowski equation

In order to solve the Smoluchowski equation, we need first to know the explicit expression of the coagulation kernel, k_{ij}, given by $k_{ij}^{Br}P_{ij}$, where k_{ij}^{Br} is the Brownian kernel [Eq. (7) with $k_{11} = 4.5 \times 10^{-12}$ m^2/s] and P_{ij} are obtained from the simulation results following the method mentioned in Sec. III B. The integration of these equations was done using a fourth-order Runge-Kutta technique with an adaptive time step [37], with $c_k(t)$ evaluated at each time step sequentially. In order to have good accuracy and reach aggregates with a mean weighted cluster size of $S_w \sim 200$, we truncated the infinite differential equations system to a set of 500 equations.

IV. RESULTS AND DISCUSSION

A. Structure

The characterization of the structure of the colloidal clusters is strongly related to the study of the aggregation kinetics. The fractal dimension characterizes the inner structure of the cluster. Is well-known that DLCA aggregation leads to more open structures ($d_f \sim 1.44$ for 2D-DLCA) than if there is some short-range repulsion between the particles such as in the RLCA regime ($d_f \sim 1.55$) [16]. However, the question that we would like to answer here is, what happens when the pairwise interaction has a repulsive component which has a range larger than the particle diameter?

We have used the radius of gyration method [1] in order to calculate the fractal dimension (Fig. 4). We observe that the slope for small sizes (before the scaling region) approaches 1 when the interaction range [Fig. 4(a)] or when V_0 [Fig. 4(b)] are increased. Although it is not possible to define the fractal dimension for the aggregates before the scaling region, this slope is clearly related to the structure of these small clusters. The approach to 1 of this slope represents an enhancement of the linear conformation of the small clusters.

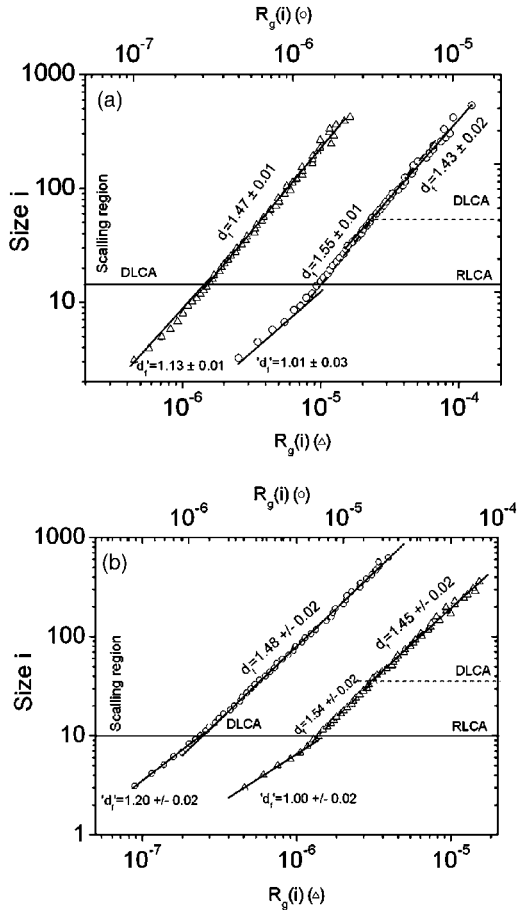

FIG. 4. The cluster size versus the radius of gyration. (a) $\kappa d=0.75$, $V_0=3k_BT$ (open circles) and $\kappa d=5$, $V_0=3k_BT$ (open triangles). (b) $\kappa d=1$, $V_0=1k_BT$ (open circles) and $\kappa d=1$, $V_0=4k_BT$ (open triangles). The slope for small aggregates approach 1 when κd decreases. The same phenomenon happens when V_0 is increased.

We also have a more direct confirmation of the high linearity of the small clusters by looking at the structure of small aggregates. In conclusion, the formation of linear structures is a consequence of the cluster-cluster repulsions, according to the discussion of Sec. II C. Indeed, a non-negligible interaction range induces an anisotropic cluster-cluster interaction potential depending on the relative orientation between the clusters. The convenient orientation to minimize the repulsion corresponds to the formation of linear structures, which means that two clusters tend to coagulate setting the monomers that constitute them as separated as possible. When the interacting clusters are large enough (larger than the critical size i_0), the cluster-cluster interaction potential becomes independent on the cluster size, as not all the monomers that form these clusters participate in the cluster-cluster interaction. From this moment, the cluster-cluster interaction potential begins to recover the isotropy and then, for these medium-sized clusters, there is not a privileged orientation of coagulation.

This important property of the cluster-cluster interactions can be easily corroborated by calculating the average interaction potential, $\langle V_{ij}\rangle$. In order to calculate $\langle V_{ij}\rangle$, 50 different clusters of size i and j where selected from the simulations,

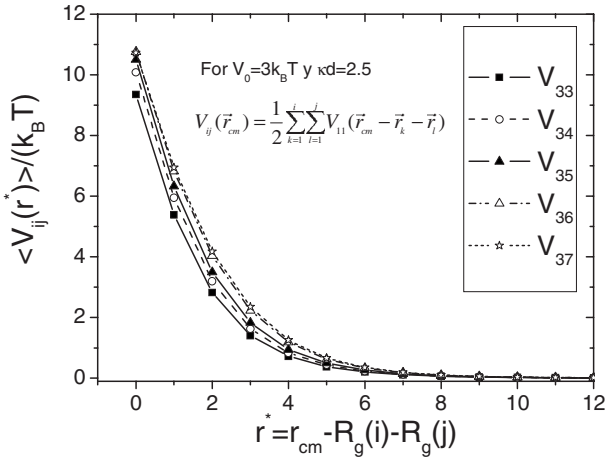

FIG. 5. Average of the trimer–i-mer interaction potential versus the cluster-cluster separation, r, where $r_{\text{c.m.}}$ is the center of mass distance and $R_g(i)$ and $R_g(j)$ the radius of gyration of the clusters, respectively. Each interaction curve is the average between a set of 50 trimers and 50 j-mers and their relative orientation. We observed that the interaction becomes more repulsive with the cluster size j. After reaching the critical size, $j=i_0=5$, the interaction becomes independent on j.

and the total interaction was averaged over their relative orientations and shapes. The $\langle V_{3j}\rangle$ interaction is shown as an example in Fig. 5 for the simulation with $V_0=3k_BT$ and $\kappa d=2.5$. We observe that the interaction potential becomes independent of j for $j\geqslant i_0=6$, which supports that the cluster reactions larger than i_0 do not depend on the clusters sizes.

When the interaction potential becomes independent of the clusters size, the effect of the interaction range becomes unimportant and the typical fractal dimension for the RLCA regime ($d_f\sim 1.55$) is recovered [see, for example, the medium region in the R_g behavior of $V_0=3k_BT$ and $\kappa d=0.75$ in Fig. 4(a) or $V_0=4k_BT$ and $\kappa d=1$ in [Fig. 4(b)].

For long enough aggregation times, the mean size of the interacting clusters is so big that there is a transition from the RLCA to the DLCA regimes as commented on in Sec. II C. Here, the coagulation process is mainly mediated by the Brownian motion of the clusters and the typical structures expected for DLCA clusters ($d_f\sim 1.44$) are recovered. This phenomenon explains the three different behaviors observed in the gyration radius in Fig. 6. For $V_0=3k_BT$ and $\kappa d>1.5$ or for $\kappa d=1$ and $V_0<2$, the RLCA region is so narrow that it cannot be distinguished.

Thus we can explain the formation of chains and the transition to the typical fractals aggregates formed in the DLCA and RLCA kinetic regimes on the basis of the superposition of the cluster-cluster interactions with a non-negligible range and the dependence of such interactions on the sizes of the involved clusters.

The formation of chain structures has been also observed in experiments [38] and simulations [40,39] in three-dimensional colloidal systems when the particles interact among them with a potential that prevents the aggregation in the primary minimum. However, this potential has a secondary minimum induced by the presence of nonadsorbing polymers (depletion interactions). This provokes a nontruly irre-

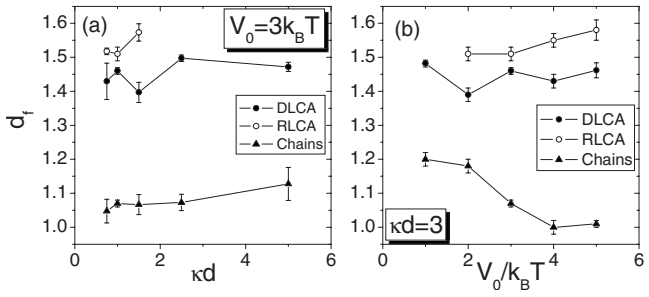

FIG. 6. (a) Fractal dimension versus κd and (b) versus V_0/k_BT. In both cases the closed triangles represent the region where the chains are formed, the closed circles describe the average cluster fractal dimension in the DLCA region, and the open circles represent the structure in the RLCA region. For $V_0=3k_BT$ and $\kappa d>1.5$ and for $\kappa d=1$ and $V_0<2$ the RLCA region cannot be distinguished.

versible aggregation. In this situation, the clusters are not rigid but they fluctuate around typical configurations and the system can be arrested as in a glass.

B. Kinetics

Figure 7 shows the evolution of the weight-average cluster size [Eq. (2)] versus the aggregation time for the simulations performed varying κd and V_0. Again, we can distinguish three different kinetic regions in the behavior of $S_w(t)$. In the first region (range effect region), the average cluster size increases very slowly with the time. Here, the growth of the clusters is strongly dependent on the parameters of the interaction potential. As can be seen in Figs. 7(a) and 7(b) this region is more clear when the interaction range or V_0 is increased. In the second region (RLCA region), the growth of the cluster is faster. Finally, in the third region (DLCA region) the average cluster size tends to the DLCA behavior. Indeed, the kinetics exponent in the third region, obtained for all the simulations performed, has the same value $z\sim0.6$, very close to the typical value of the kinetic exponent for the DLCA aggregation regime ($z_{DLCA}=0.59$ [16]).

The kinetic results of the simulations are consistent with the effect of the interaction range considered in Sec. II C. For small aggregates (with sizes $i<i_0$) the cluster-cluster repulsion increases with the cluster size. This explains the first kinetic region where the growth of the clusters is very slow. When the mean cluster size is about the critical size, i_0, the interaction becomes size-independent of the size, i.e., the effect of the interaction range becomes negligible. Therefore aggregation rate is faster due to the increase of the cross section of the clusters, keeping the interaction potential constant: this is the RLCA region. When the aggregates are large enough, every encounter between clusters provokes coagulation after some time. So, a DLCA regime displaced in time is recovered, and the kinetic exponent approaches the typical for the DLCA regime ($z\sim0.59$).

C. Coagulation kernels

The aggregation rate constants k_{ij} account for all the relevant physical and chemical effects on the kinetics of the aggregation process. The influence of the pairwise interaction potential between the particles over the coagulation kinetics is resumed in the P_{ij} function ($k_{ij}=k_{ij}^{Br}P_{ij}$). Thus all the effects of the interaction potential over the kinetics of the coagulation processes have been included in the P_{ij} functions. As we see in Sec. III B, we have developed a method to obtain these functions directly from the simulations, and then, this allows us to analyze the effect of the interactions over the coagulation kinetic.

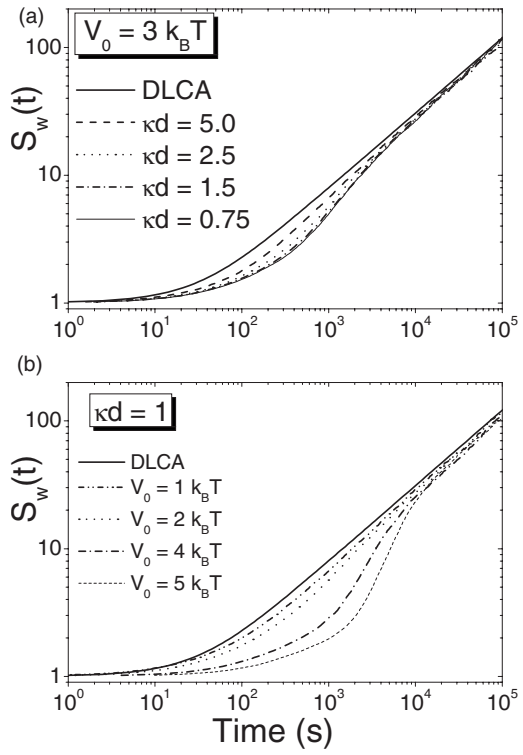

FIG. 7. Weight cluster size for the different simulations performed

In Fig. 8 we show the P_{ij} obtained in the simulations versus the sizes of the reacting clusters i and j when the particles interact with a Yukawa potential with $V_0=3k_BT$ for the studied values of κd. For the shorter interaction range

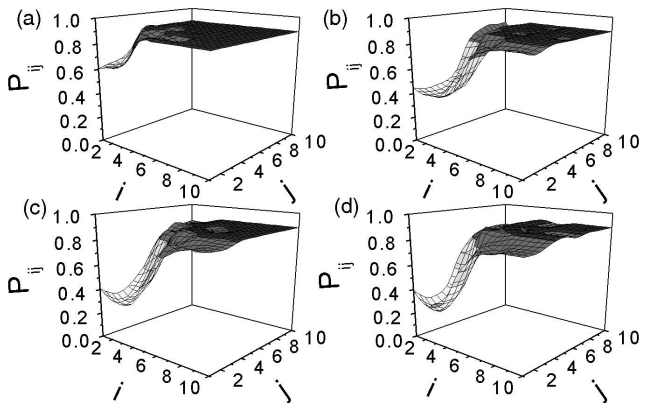

FIG. 8. P_{ij} functions obtained from the simulations for the values of the interaction potential $V_0=3k_BT$ and (a) $\kappa d=5$, (b) $\kappa d=2.5$, (c) $\kappa d=1.5$, and (d) $\kappa d=0.75$.

[Fig. 8(a) with $\kappa d=5$], the kernel increases with i and j until it reaches a constant value. In this case, the range of the interaction is very short and the cluster-cluster interaction potential V_{ij} does not depend on the clusters sizes so the effect of the interaction range is irrelevant. The P_{ij} functions increase with the cluster sizes i and j because the number of particles that can collide in the encounter between these aggregates increases with their sizes. This is the typical RLCA aggregation regime where the kernel is given by Eq. (10). Finally, when the sizes of the reacting aggregates are very large, their diffusion coefficients are very small and they have more probability to interact between them many times than diffuse and interact with another cluster. Hence the crossover to DLCA appears. However there is a time between the beginning of the encounter and the coagulation which causes that the pure DLCA regime cannot be reached. Hence in this region $k_{ij}=Ak_{ij}^{Br}$ where A is a constant less than 1.

If the interaction range is enlarged, the cluster-cluster interaction potential becomes more repulsive when the sizes of the involved clusters are increased. This causes the decrease of P_{ij} with i and j for small clusters. This effect can be clearly observed in Figs. 8(b)–(d) where $\kappa d=2.5$, 1.5, and 0.75, respectively. For large enough aggregates $(i,j \geqslant i_0)$, V_{ij} becomes independent on i and j so the RLCA coagulation regime is found and the functions P_{ij} start growing with the cluster's sizes. Finally, for large aggregates, the coagulation process is mediated again by the diffusion of the clusters and the third region appears in the behavior of P_{ij}, where this functions remains constant with i and j.

The quantitative dependencies of the P_{ij} functions with the interaction range κd are shown in Fig. 9. Each inset shows P_{ij} versus i for a fix j and for the simulations with $V_0=3k_BT$ and $\kappa d=0.75$, 1.5, 2.5, and 5. Here, the three different kinetic regions (effect of the interaction range, RLCA, and DLCA) can be clearly observed. The curvature of P_{ij} for small values of i and j is enhanced for long range repulsions. This is due to the growth of the critical size i_0 with the interaction range. For sizes bigger than i_0, the interaction potential V_{ij} becomes independent of the clusters sizes and the RLCA regime is recovered. Finally, the functions P_{ij} tend again to a saturation value P_∞ for large values of i and j. This value is the same for all the simulations performed with $V_0=3k_BT$ so P_∞ is independent of the interaction range.

In Fig. 10 we present the P_{ij} obtained from the simulations with $\kappa d=1$ and for the different values of V_0 used. For these simulations we always observe the three different kinetic regions (interaction range-RLCA-DLCA). We also show, in Fig. 11, the effect of varying V_0 in the same plot on P_{ij}, with i fixed in each of the insets. The functions P_{ij} also tend to a saturation value P_∞ for large values of i and j, but in this case this value depends on the value of the V_0 used in the simulations. This can be explained by the fact that the effect of the interaction range becomes negligible in the P_{ij} functions when the sizes i and j are very large. Therefore the magnitude that determines the values of these functions for $i,j \gg 1$ is the interaction potential at contact, that is, V_0. Greater values of V_0 imply smaller values of the coagulation probability by collision, and then, smaller values for P_∞. This can be understood with the idea that for large aggregates all the encounters end up in a coagulation, but there is a finite time between the beginning of the encounter and the coagulation, this time being determined by V_0.

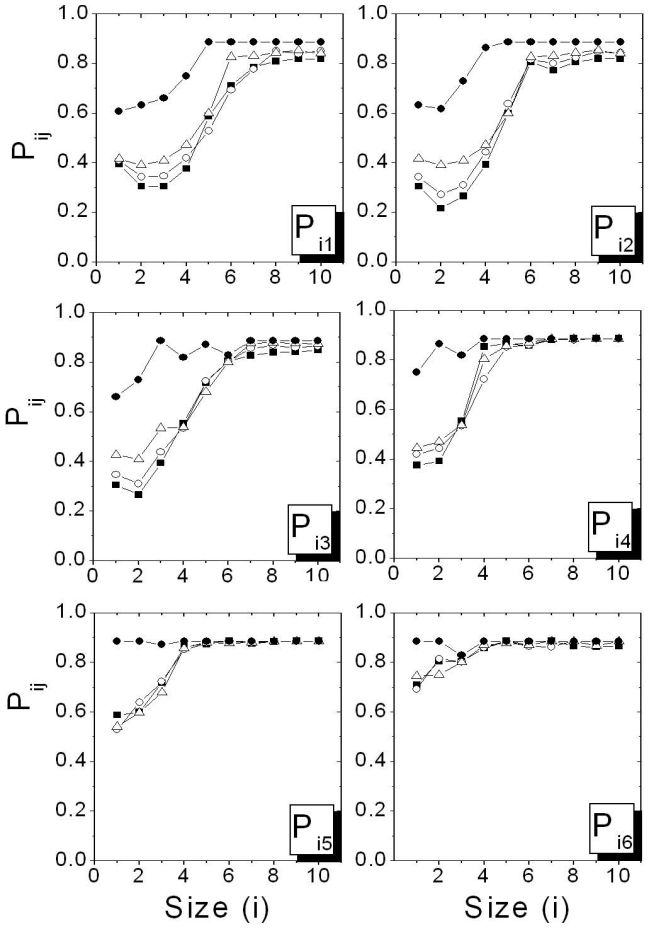

FIG. 9. In each inset we represent the P_{ij} functions for j fixed (j from 1 to 6) versus i for $V_0=3k_BT$ and for all values of κd used in the simulations (closed squares, $\kappa d=0.75$; open circles, $\kappa d=1.5$; open triangles, $\kappa d=2.5$; and closed circles, $\kappa d=5.0$).

By solving the Smoluchowski equation [Eq. (3)] with these aggregations kernels we are able to reproduce the clus-

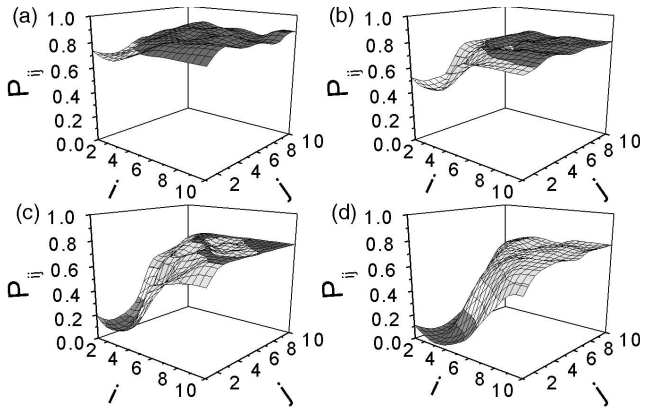

FIG. 10. P_{ij} functions obtained from the simulations for the values of the interaction range $\kappa d=1$ and (a) $V_0=1k_BT$, (b) $V_0=2k_BT$, (c) $V_0=4k_BT$, and (d) $V_0=5k_BT$.

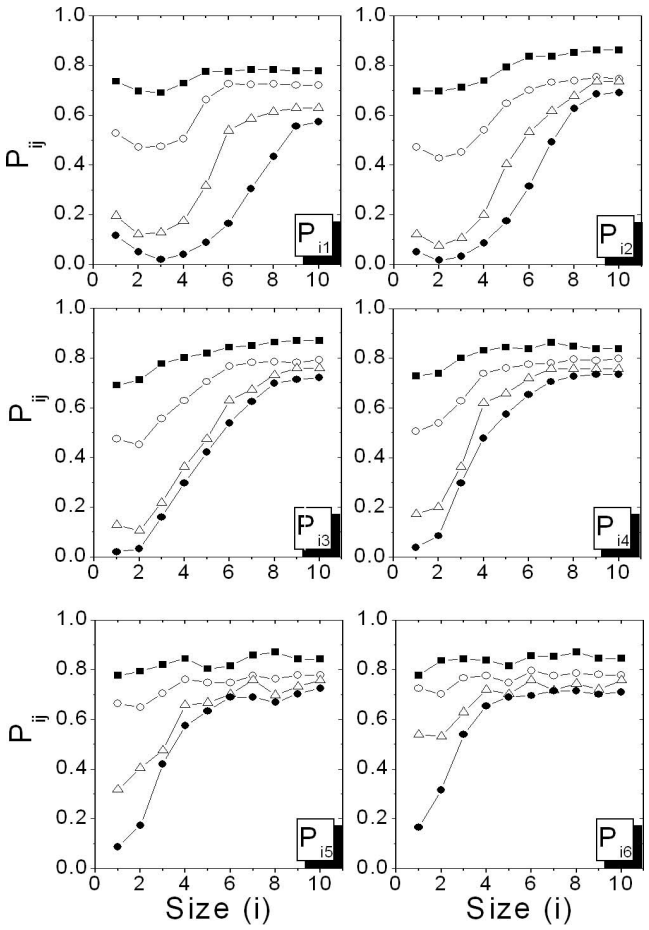

FIG. 11. In each inset we represent the P_{ij} functions for j fix (j from 1 to 6) versus i for $\kappa d=1$ and for all values of V_0 used in the simulations (closed squares, $V_0=1k_BT$; open circles, $V_0=2k_BT$; open triangles, $V_0=4k_BT$; and closed circles, $V_0=5k_BT$).

ter size distributions and the weighted average cluster size with good accuracy for all the simulations (Fig. 12).

Therefore we are able to characterize the coagulation kinetics through the P_{ij} functions where the transition between the three kinetic regions is included. When the mean cluster size reaches the defined critical size, i_0, the transition from the first kinetic regime (induced by the range of the interaction) to the classical kinetic regimes (RLCA and DLCA) appears.

V. CONCLUSIONS

We studied the effect of an interaction potential with a non-negligible range on the kinetic properties and the structure of the aggregates formed in a computer-simulated two-dimensional aggregating system.

Three different regions have been observed in the representation of the weight-average cluster size $S_w(t)$ that corresponds with three kinetics regions. "Interaction range region:" here the cluster-cluster interaction potential, V_{ij}, becomes more repulsive with the increasing of the sizes of the clusters due to the non-negligible range of the interaction. In this region, the aggregates tend to adopt a linear structure. This phenomenon is contrasted with the direct observation of the small aggregates given by the simulations. The linearity of the small aggregates can be explained based on the "superposition approximation" of the interaction potential. RLCA region: when the reacting clusters have sizes over the critical size i_0, not all the monomers that compose these aggregates participate in the total interaction. Therefore V_{ij} becomes independent on i and j for $i,j>i_0$, the cluster-cluster interaction recovers its isotropy. From this time, the classical aggregation kinetics are recovered with the well-known RLCA-DLCA crossover. The chains formed in the previous region coagulate to form fractal aggregates with a fractal dimension typical for the RLCA coagulation. In this region, the growing of the clusters is faster than in the previous region. "DLCA region:" here, the diffusion coefficients of the reacting clusters are very low and so it is easier for two interacting large clusters to collide between them many times and coagulate than to diffuse away to collide with another cluster. Hence for large aggregates all "encounters" between two aggregates end up in coagulation after some time and the coagulation limited by the Brownian diffusion of the clusters (DLCA) is recovered, which explains the fractal dimension of the aggregates formed after the scaling time typical for DLCA obtained in all simulations.

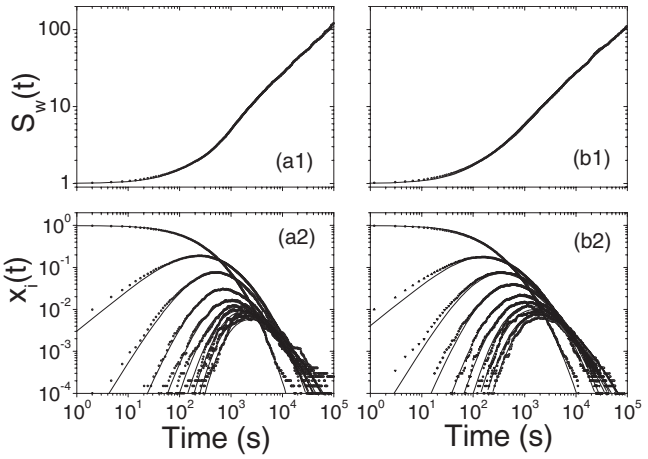

FIG. 12. Weight-average cluster size $S_w(t)$ and cluster sizes distribution $x_i(t)=n_i(t)/N_0$ given by the simulations (open circles) and the results of solving the Smoluchowski equation (3) (lines) with the obtained kernels for (a1) and (a2) $V_0=3k_BT$ and $\kappa d=0.75$; and (b1) and (b2) $V_0=2k_BT$ and $\kappa d=1$.

A method has been developed in order to obtain the aggregation rate constants through the functions $P_{ij}=k_{ij}/k_{ij}^{Br}$ directly from the simulations performed. This method allows us to study the effect of the interaction range over the real coagulation kinetics. Then, the kernel found with this procedure was introduced in the Smoluchowski equation (3) and the cluster size distributions were obtained. These functions were compared with the simulation and the adjustment is practically perfect.

Therefore we have connected the kinetic region induced by the range of the interaction with the well-known RLCA-DLCA crossover. Hence we have a complete description of the kinetic behavior of a two-dimensional aggregating sys-

tem composed by colloidal particles that interact with a medium-range pairwise repulsive interaction. We have observed that the range of the interaction modifies not only the kinetics of the coagulation process at short times but also the structure of the small aggregates formed in this process. Moreover, although the effect of the interaction range appears only in the first stages of the coagulation, the consequences of this affect the complete development of the process.

Future investigations will involve the study of the effect of the interaction range in a three-dimensional coagulation process, where we are able to calculate theoretically the "stability factor."

ACKNOWLEDGMENTS

Financial support from Ministerio de Educación y Ciencia [Plan Nacional de Investigación Científica, Desarrollo e Innovación Tecnológica (I+D+i), Project No. MAT2006-12918-C05-01], by the European Regional Development Fund (ERDF), by Project No. FQM 392 from Junta de Andalucía, and the DGAPA/UNAM (Proyecto PAPIIT IN118705-2) are gratefully acknowledged.

[1] J. Maldonado-Valderrama, V. B. Fainerman, E. Aksenenko, M. J. Gálvez-Ruiz, M. A. Cabrerizo-Vílchez, and R. Miller, Colloids Surf., A **261**, 8592 (2005).
[2] C. Haro-Pérez, M. Quesada-Pérez, J. Callejas-Fernández, E. Casals, J. Estelrich, and R. Hidalgo-Álvarez, J. Chem. Phys. **118**, 5167 (2003).
[3] J. M. Rubí, and A. Pérez-Madrid, Physica A **298**, 177 (2001).
[4] M. J. Santander-Ortega, A. B. Jódar-Reyes, N. Csabac, D. Bastos-González, and J. L. Ortega-Vinuesa, J. Colloid Interface Sci. **302**, 522 (2006).
[5] S. Melle, M. A. Rubio, and G. G. Fuller, Phys. Rev. Lett. **87**, 115501 (2001).
[6] E. H. A. de Hoog, W. K. Kegel, A. van Blaaderen, and H. N. W. Lekkerkerker, Phys. Rev. E **64**, 021407 (2001).
[7] M. Brunner, J. Dobnikar, H. H. von Grünberg, and C. Bechinger, Phys. Rev. Lett. **92**, 078301 (2004).
[8] J. Silk and S. D. M. White, Astrophys. J. **223**, L59 (1978); J. D. Barrow, J. Phys. A **14**, 729 (1981).
[9] M. V. Smoluchowski, Phys. Z. **17**, 557 (1916).
[10] P. Meakin, Phys. Scr. **46**, 295 (1992).
[11] F. Leyvraz, Phys. Rep. **383**, 95 (2003).
[12] F. Family, P. Meakin, and T. Vicsek, J. Chem. Phys. **83**, 4144 (1985).
[13] M. Kolb and R. Jullien, J. Phys. (France) Lett. **45**, L977 (1984).
[14] A. E. González, F. Martínez-López, A. Moncho-Jordá, and R. Hidalgo-Álvarez, Physica A **333**, 257 (2003).
[15] A. J. Hurd and D. W. Schaefer, Phys. Rev. Lett. **54**, 1043 (1983).
[16] A. Moncho-Jordá, G. Odriozola, F. Martínez-López, A. Schmitt, and R. Hidalgo-Álvarez, Eur. Phys. J. E **5**, 471 (2001).
[17] T. Vicsek and F. Family, Phys. Rev. Lett. **52**, 1669 (1984).
[18] P. Meakin, T. Vicsek, and F. Family, Phys. Rev. B **31**, 564 (1985).
[19] G. Odriozola, A. Moncho-Jordá, A. Schmitt, J. Callejas-Fernández, R. Martínez-García, and R. Hidalgo-Álvarez, Europhys. Lett. **53**, 797 (2001).
[20] R. L. Drake, *Topics in Current Aerosol Research (Part 2)*, edited by G. M. Hidy and J. R. Brock (Oxford, Pergamon, 1972), p. 201376.
[21] M. H. Ernst, *Kinetics of Clustering in Irreversible Aggregation Fractals in Physics*, edited by L. Pietronero and E. Tosatti (North-Holland, Amsterdam 1986), p. 289302.
[22] R. Jullien and R. Botet, *Aggregation and Fractal Aggregates* (World Scientific, Singapore, 1987).
[23] M. H. Lee, Astrophys. J. **418**, 147162 (1993).
[24] G. Odriozola, A. Schmitt, A. Moncho-Jordá, J. Callejas-Fernandez, R. Martínez-Garcia, R. Leone, and R. Hidalgo-Álvarez, Phys. Rev. E **65**, 031405 (2002).
[25] T. Sintes, R. Toral, and A. Chakrabarti, Phys. Rev. E **50**, 2967 (1994).
[26] M. H. Ernst and P. G. J. van Dongen, Phys. Rev. A **36**, 435 (1987).
[27] A. A. Lushnikov, Phys. Rev. E **73**, 036111 (2006).
[28] R. Jullien, Croat. Chem. Acta **65**, 215 (1992).
[29] T. Vicsek, *Fractal Growth Phenomena* (World Scientific, Singapore, 1992).
[30] N. Fuchs, Z. Phys. **89**, 736 (1934).
[31] M. Y. Lin, H. M. Lindsay, D. A. Weitz, R. C. Ball, R. Klein, and P. Meakin, Phys. Rev. A **41**, 2005 (1990).
[32] C. Cametti, P. Codastefano, and P. Tartaglia, J. Colloid Interface Sci. **131**, 409 (1989).
[33] A. Di Biasio, G. Bolle, C. Cametti, P. Codastefano, F. Sciortino, and P. Tartaglia, Phys. Rev. E **50**, 1649 (1994).
[34] J. K. G. Dhont, *An Introduction to Dynamics of Colloids* (Elsevier, Amsterdam, 1996).
[35] A. Moncho-Jordá, F. Martínez-López, and R. Hidalgo-Álvarez, Physica A **282**, 50 (2000).
[36] J. C. Fernández-Toledano, A. Moncho-Jordá, F. Martínez-López, A. E. González, and R. Hidalgo-Álvarez, Phys. Rev. E **71**, 041401 (2005).
[37] W. H. Press, S. A. Teulkolsky, W. T. Vettering, and B. P. Flannery, *Numerical Recipes*, 2nd ed. (Cambridge University Press, Cambridge, England, 1992).
[38] A. I. Campbell, V. J. Anderson, J. S. van Duijneveldt, and P. Bartlett, Phys. Rev. Lett. **94**, 208301 (2005).
[39] F. Sciortino, P. Tartaglia, and E. Zaccarelli, J. Phys. Chem. B **109**, 21942 (2005).
[40] A. de Candia, E. Del Gado, A. Fierro, N. Sator, and A. Coniglio, Physica A **358**, 239 (2005).